ELSEVIER

Journal of Nuclear Materials 313–316 (2003) 1202–1205

journal of nuclear materials

www.elsevier.com/locate/jnucmat

Unified analytic representation of hydrocarbon impurity collision cross-sections

R.K. Janev [a,b], D. Reiter [a,*]

[a] *Institut für Plasmaphysik, Forschungszentrum-Jülich GmbH, EURATOM Association, Trilateral Euregio Cluster, D-52425 Jülich, Germany*

[b] *Macedonian Academy of Sciences and Arts, P.O. Box 428, 1000 Skopje, Macedonia*

Abstract

The available experimental information and semi-empirical scaling properties on total cross-sections for electron impact ionization, dissociative excitation and recombination processes of hydrocarbon molecules and their ions, as well as for proton charge exchange on these molecules, were used to derive unified analytic representations of these cross-sections for all C_xH_y molecules and their ions with $x = 1$–3 and $1 \leqslant y \leqslant 2x + 2$. The procedure for obtaining the partial cross-sections for individual reaction channels of a given process from the presented total cross-sections is outlined.

PACS: 52.40.H
Keywords: Plasma–wall interactions; Boundary plasmas; Carbon; Hydrocarbons; EIRENE code

1. Introduction

Because of its low atomic number (i.e. low radiative capacity) and its capability to withstand high heat fluxes, carbon (in form of graphite or carbon–carbon composites) continues to be used as plasma facing material in most presently operating fusion devices (e.g. JET, JT-60U, D-III D, LHD, ASDEX-U, TEXTOR, etc.), and it is the leading candidate for such materials in the divertor designs of next-generation fusion machines.

This is the case despite one of the most critical current design problems for fusion devices is related to this material, namely the carbon re-deposition and tritium co-deposition problem. On JET, operated with tritium, the tritium inventory was found to build up without saturation limit.

This problem may be so serious as to rule out the use of carbon in fusion devices. That would, however, eliminate the material that, by a considerable margin, we know most about. It therefore would be a setback for fusion research driven to the extreme [1].

There are several sub-components to this problem, such as large scale convection in the SOL, the source of carbon at the walls, and the plasma chemistry and neutral hydrocarbon transport. In order to separate the first two of these from the third, by means of numerical plasma edge simulation codes, a detailed and accurate knowledge of the cross-sections of the relevant plasma chemical processes is required.

A systematic effort has recently been undertaken [2–6] to compile, critically assess and generate the cross-sections for all important collision processes of hydrocarbon molecules C_xH_y ($x = 1$–3; $1 \leqslant y \leqslant 2x + 2$) and their ions with plasma electrons and protons. These processes include: direct and dissociative ionization, excitation and recombination of C_xH_y and $C_xH_y^+$ in collisions with electrons, and charge and particle exchange of C_xH_y with protons.

In the course of that work certain cross-section scaling relationships have been revealed, and used to generate cross-section data for those collision systems for which such data were not available in the literature.

* Corresponding author. Tel.: +49-2461 615841; fax: +49-2461 612970.
E-mail address: d.reiter@fz-juelich.de (D. Reiter).

0022-3115/03/$ - see front matter
PII: S0022-3115(02)01569-6

In the present work we shall use the available experimental cross-section data and the observed cross-section scaling relationships to obtain a unified analytic representation of the cross-sections of a given process for all hydrocarbon molecules or molecular ions with $x = 1$–3 and $1 \leqslant y \leqslant 2x + 2$. For majority of considered processes, it is also possible to suggest a procedure for obtaining approximately the cross-sections for the individual reaction channels from the total ones.

The full set of individual processes and cross-section data for hydrocarbon breakup in divertor plasmas is so large that it may require bulky Monte Carlo simulation codes. The unified expressions and scaling relations given in the present paper can greatly simplify this, and may even render a simple analytical assessment possible.

2. Electron processes with C_xH_y and $C_xH_y^+$

We shall consider the following electron impact processes

(1) Direct (I) and dissociative (DI) ionisation of C_xH_y:

$$e + C_xH_y \rightarrow C_xH_y^+ + 2e \tag{1a}$$

$$\rightarrow C_{x-k}H_{y-l} + C_{x'}H_{y'}^+ + \sum_{\kappa,\lambda}^{k-x',l-y'} C_\kappa H_\lambda + 2e \tag{1b}$$

(2) Dissociative excitation (DE) of C_xH_y neutrals:

$$e + C_xH_y \rightarrow C_{x-k}H_{y-l} + \sum_{\kappa,\lambda}^{k,l} C_\kappa H_\lambda + e \tag{2}$$

(3) Dissociative excitation (DE) of $C_xH_y^+$ ions:

$$e + C_xH_y^+ \rightarrow C_{x-k}H_{y-l}^+ + \sum_{\kappa,\lambda}^{k,l} C_\kappa H_\lambda + e \tag{3}$$

(4) Dissociative recombination (DR):

$$e + C_xH_y^+ \rightarrow \sum_{\kappa,\lambda}^{x,y} C_\kappa H_\lambda \tag{4}$$

where the summations in (1)–(4) go over all fragmentation channels.

The processes of dissociative ionisation of $C_xH_y^+$ ions have much higher energy thresholds ($E_{th} \geqslant 25$ eV) than the dissociative excitation to neutrals ($E_{th} \sim 10$ eV) and, at least in cold divertor plasmas, their role is expected to be less important.

The ionization and dissociation processes (1)–(3) all proceed via similar dynamical mechanisms. The energy dependence of their cross-sections is characterized by a sharp, power-law increase near the threshold, and a Born – type behavior at high collision energies. On the other hand, distinct scaling properties can be observed for the cross-sections for all these three classes of processes with respect to the number of C and H atoms in the C_xH_y molecule (or molecular ion) [3–7]. These cross-section scaling relationships can be related [7,3–6] to the 'additivity rules' for the strengths of the chemical bonds in complex molecules [8] which show an extraordinary 'stability' with respect to external perturbations (e.g. multipole induced interactions, etc.). Since these additivity rules do not have a dynamical origin and are related to the molecular structure only, one is tempted to separate out the structural and dynamical parts in the total cross-section for a given process. In order to achieve a unified representation of the energy dependent dynamical part of the cross-section, it is necessary to introduce a reduced energy variable, $\varepsilon = E/E_{th}$, where E is the collision energy and E_{th} is the threshold energy for the reaction. The factored form of the total cross-section for any of the processes (1)–(3) can then be written as

$$\sigma_\lambda^{tot}(x,y) = F_\lambda(x,y)\frac{A_\lambda}{E_{th}}\left(1 - \frac{1}{\varepsilon}\right)^{\alpha_\lambda} \times \frac{1}{\varepsilon}\ln(e + a_\lambda\varepsilon)(\times 10^{-16}\ \text{cm}^2), \tag{5}$$

where λ indicates the reaction type ($\lambda = 1,2,3$ for the processes (1)–(3), respectively), A_λ, α_λ and a_λ are parameters of the dynamical part of the cross-section, $F_\lambda(x,y)$ is the 'structural' part of the cross-section and $e = 2.71828\ldots$ is the base of natural logarithm (introduced for convenience). The threshold energy E_{th} (expressed in units of eV) in Eq. (5) appears due to the transition from E to ε in a Born-type expression for the cross-section. Thus, the reduced cross-section $\bar{\sigma}_\lambda^{tot}(\varepsilon) = \sigma_\lambda^{tot}(x,y)E_{th}/F_\lambda(x,y)$ defines a 'universal' cross-section for a given process λ.

Guided by the observed semi-empirical cross-section scaling relationships, and using the available data for the total cross-sections of reactions (1)–(3) [3–6], we obtain (by simple fitting procedures) for $F_\lambda(x,y)$ the expressions

$$F_1(x,y) = (1 + 0.373y) + 0.47(x-1) \times \left[\left(1 + \frac{x + 5.65}{x}\right) - \frac{0.655y(1-\delta_{x,1})}{(x-1)}\right], \tag{6}$$

$$F_2(x,y) = (1 + 0.29y) + 1.25(x-1) \times \left[0.25(x-1) - \frac{0.36y}{x^2}\right], \tag{7}$$

$$F_3(x,y) = 1 + 0.71(y-1) + (x-1) \times \left[0.45 + \frac{0.19y(1-\delta_{x,1})}{x-1}\right], \tag{8}$$

where $\delta_{x,1}$ is the Kronecker symbol. The parameters A_λ, α_λ and $a_\lambda$have the following values: $A_{1;2;3} = 84.0$; 34.6; 29.4, $\alpha_{1;2;3} = 3.0$; 3.0; 2.5, $a_{1;2;3} = 0.96$; 1.27; 7.02. The values of the remaining parameter E_{th} in Eq. (5) can be

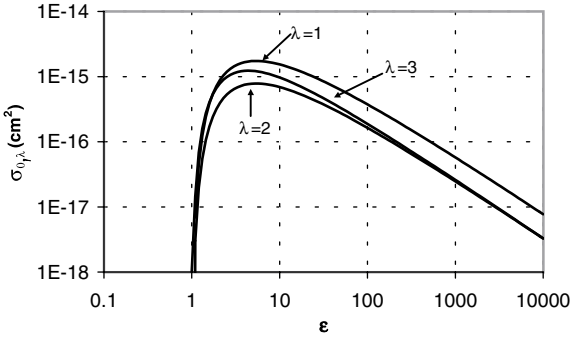

Fig. 1. Reduced total cross-sections $\tilde{\sigma}_\lambda$ for electron-impact ionization ($\lambda = 1$), dissociative excitation of C_xH_y ($\lambda = 2$), and dissociative excitation of $C_xH_y^+$ ($\lambda = 3$) as function of reduced collision energy $\varepsilon = E/E_{\rm th}$.

found elsewhere [3–6,9]. The reduced (universal) cross-sections $\tilde{\sigma}_\lambda(\varepsilon)$ for $\lambda = 1, 2, 3$ are shown in Fig. 1. The estimated accuracy of total cross-sections represented by the analytical formula (5) are: for $\lambda = 1$: better than 20% for $x = 1$, 50% for $x = 2$, 70% for $x = 3$; for $\lambda = 2$: better than 70% (for all x) and $\lambda = 3$: better than 50%.

The process of dissociative recombination of $C_xH_y^+$ ions with electrons has a quite different physical nature than the processes (1)–(3): it is an exothermic process, and its cross-section at thermal energies obeys the Wigner E^{-1} – law. Resonance structures in the cross-section and the competing process (3) introduce deviations of the cross-section $\sigma_{\rm DR}$ for these reactions from the E^{-1} behavior at energies above ~5 eV. Except for the CH_y^+ ions, for which direct cross-section measurements on $\sigma_{\rm DR}$ exist, the experimental data are available only for the reaction rate coefficients for these systems, and most frequently in the thermal temperature region [5,6]. The dissociative recombination rate coefficients $\langle v\sigma_{\rm DR}\rangle$ for $C_xH_y^+$ show distinct linear dependencies on x and y. By fitting the assessed experimental rate coefficients [5,6] to an expression having a $T^{-1/2}$ behaviour at low T (consistent with the E^{-1} cross-section dependence at thermal energies), we obtain

$$\langle v\sigma_{\rm DR}\rangle(C_xH_y^+) = F_4(x,y)T^{-1/2}(1+0.27T^{0.55})^{-1} \times (\times 10^{-8}\ \mathrm{cm^3/s}), \tag{9}$$

$$F_4(x,y) = 0.415\left[1+6.48(x-1)\left(1+\frac{1.75(x-2)}{x^2}\right)\right] + 0.83\left[1+\frac{0.776(x-1)}{(x-0.95)^{2.62}}\right]y \tag{10}$$

and electron temperature T in Eq. (9) is expressed in eV. The validity of Eq. (9) extends up to about ~20–30 eV with an accuracy better than 30–40%.

3. Proton charge exchange with C_xH_y

The proton charge exchange reaction with C_xH_y molecules provides another important type of processes (labeled (5) here). It has two main channels

(5) Charge exchange and particle rearrangement (CX):

$$H^+ + C_xH_y \to H + C_xH_y^+ \tag{11a}$$

$$\to H_2 + C_xH_{y-1}^+ \tag{11b}$$

The heavy particle rearrangement channel (11b) is important only in the thermal energy region, while for energies above ~0.5 eV the electron capture (or, pure charge exchange) channel dominates. The database for reactions 11a,11b has been analyzed in [2,5,6] in detail. The pure charge exchange reactions in these collision systems can be divided into two groups: resonant (when $2x-1 \leqslant y \leqslant 2x+2$ for $x = 2$, 3; and $y = 3$, 4 for $x = 1$) and non-resonant reactions [2]. The cross-sections of resonant reactions in the region bellow ~15 keV/amu (atomic mass unit) slowly increase with decreasing of collision energy down to thermal energies. The cross-sections of non-resonant reactions have a broad maximum around ~10–15 keV/amu, and with decreasing the energy they pass through a minimum after which they start again to increase towards their thermal energy values (determined by the polarization capture mechanism for the process). The cross-sections of non-resonant charge exchange reactions in the energy region below their maxima are rather sensitive to the electronic structure of the collision system (the collisional dynamics is governed by strong coupling of many electronic states of the entire collision system) and, in absence of a single dominant mechanism for the process, no general cross-section scaling relationship can be expected. In contrast to this, the electron capture in the case of resonant reactions is governed (in the energy region bellow ~10 keV/amu) by an electron tunneling mechanism, which allow simple (still approximate) theoretical description and, on its basis, revealing of scaling parameters for the process (and its cross-section). By using the assessed cross-section data from Refs. [2,5,6], and limiting the collision energy to the range $0.1 \leqslant E(\mathrm{eV}) \leqslant 10^4$, the cross-sections of resonant charge exchange reactions can be represented in the form

$$\sigma_{\rm CX,res}^{\rm tot}(C_xH_y) = 2.76\frac{Ry}{I_p}y^{1/2}E^{-0.14}(\times 10^{-15}\ \mathrm{cm^2}), \tag{12}$$

where $Ry = 13.605$ eV is the Rydberg energy and E is expressed in eV units. The reduced resonant charge exchange cross-section,

$$\tilde{\sigma}_{\rm CX,res}^{\rm tot} = \frac{I_p/Ry}{y^{1/2}}\cdot\sigma_{\rm CX,res}^{\rm tot} \tag{13}$$

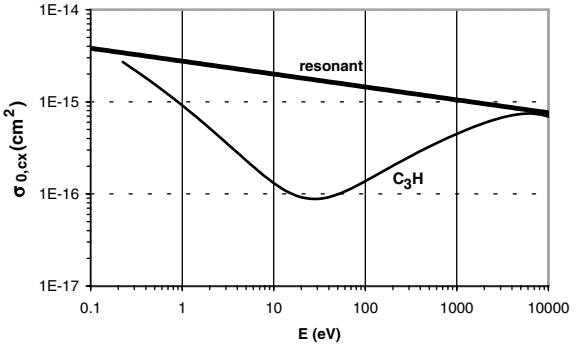

Fig. 2. Reduced total cross-section $\tilde{\sigma}^{\rm tot}_{\rm CX,res}$ for 'resonant' $H^+ + C_xH_y$ charge exchange reactions as function of collision energy (thick line). The thin line shows the behaviour of $\tilde{\sigma}^{\rm tot}_{\rm CX}$ for a typical non-resonant charge exchange reaction: $H^+ + C_3H \rightarrow H + C_3H^+$.

as function of E is shown in Fig. 2. Also included in this figure (lower line) is the $\tilde{\sigma}^{\rm tot}_{\rm CX}$ for a typical non-resonant CX reaction: $H^+ + C_3H \rightarrow H + C_3H^+$.

The accuracy of the cross-sections represented by Eq. (12) is better than 15% in the indicated energy range. For non-resonant charge exchange reactions one can use the more complicated analytic fits for the cross-sections given in [2,5,6].

4. Partial cross-sections

As indicated by Eqs. (1)–(4), all electron impact processes of C_xH_y and $C_xH_y^+$ have many exit reaction channels, the number of which increases with increasing x and y. It has been observed [3,10] that the fractional contribution of exit reaction channels in the process (1a), (1b) to the total cross-section is energy invariant for $E \geqslant 30$–40 eV. It was argued in Refs. [5,6] that such energy invariance holds also for the reaction branching ratios of processes (2) and (3). For the process (4), the energy invariance of the branching ratios up to energies 1–2 eV can be expected from the very break-up mechanism (the Wigner E^{-1}-law). Therefore, in the specified energy regions, the partial cross-section σ^j_λ for a particular reaction channel j of the process λ ($\lambda = 1$–4) can be written as

$$\sigma^j_\lambda = R^j_\lambda \sigma^{\rm tot}_\lambda, \quad \lambda = 1 - 4. \tag{14}$$

The two (main) reaction channels of the charge exchange process 11a,11b are of comparable importance only in the energy region bellow ~0.1 eV and their branching ratio is energy independent only at thermal energies. The values of R^j_λ for $\lambda = 1$–4 can be found in [3–6], while for $\lambda = 5$ in [2]. Within an accuracy of factor of two or better, the values of R^j_λ for $\lambda = 1$–3 can be extended down to the threshold, while those for R^j_4 up to 3–5 eV.

5. Conclusion

We have provided unified analytic formulae for total cross-sections of processes (1)–(3), total rate coefficients of dissociative recombination (4), and total cross-sections of resonant reactions of charge exchange process (11a). The construction of these formulae was based on the use of established semi-empirical cross-section scaling relationships and the available cross-section data. Only in the case of non-resonant reactions of the process (11a) a unified cross-section representation could not be derived.

Within an accuracy of factor of two or better, one can obtain from the provided total cross-sections also the partial cross-sections for individual reaction channels in processes (1)–(4) by using the relation (14).

References

[1] P.C. Stangeby, Some observations about the current state of edge plasma physics, presented at IAEA TCM on divertor concepts, Aix-en-Provence, France, September 2001.
[2] R.K. Janev, J.G. Wang, T. Kato, National Institute of Fusion Science (Toki) Report NIFS-DATA-64, 2001.
[3] R.K. Janev, J.G. Wang, I. Murakami, T. Kato, National Institute of Fusion Science (Toki) Report NIFS-DATA-68, 2001.
[4] R.K. Janev, D. Reiter, Phys. Plasmas 9 (2002) 4071.
[5] R.K. Janev, D. Reiter, FZJ (Forschungszentrum Jülich) Report Juel-3966, February 2002.
[6] R.K. Janev, D. Reiter, FZJ (Forschungszentrum Jülich) Report Juel-4005, October 2002.
[7] B.L. Schram, M.J. van der Wiel, F.J. de Heer, H.R. Moustafa, J. Chem. Phys. 44 (1966) 49.
[8] S.W. Benson, J.H. Buss, J. Chem. Phys. 29 (1958) 546.
[9] H.M. Rosenstock, K. Draxl, et al., J. Phys. Chem. Ref. Data 6 (Suppl. 1) (1977).
[10] C.E. Melton, J. Chem. Phys. 37 (1962) 139.